AWARD NUMBER: W81XWH-18-1-0102

TITLE: Emerging Infectious Disease Diagnostic via Novel Optoelectronic Halo Effect

PRINCIPAL INVESTIGATOR: Michael J. Naughton

CONTRACTING ORGANIZATION: Boston College, Chestnut Hill, MA

REPORT DATE: February 2022

TYPE OF REPORT: Final

PREPARED FOR: U.S. Army Medical Research and Development Command
Fort Detrick, Maryland 21702-5012

REPORT DOCUMENTATION PAGE

Form Approved
OMB No. 0704-0188

1. REPORT DATE	**2. REPORT TYPE**	**3. DATES COVERED**
February 2022	Final	15Apr2018 – 14Oct2021

4. TITLE AND SUBTITLE

Emerging Infectious Disease Diagnostic via Novel Optoelectronic Halo Effect

5a. CONTRACT NUMBER
W81XWH-18-1-0102

5b. GRANT NUMBER

5c. PROGRAM ELEMENT NUMBER

6. AUTHOR(S)
Michael J. Naughton

E-Mail: naughton@bc.edu

5d. PROJECT NUMBER

5e. TASK NUMBER

5f. WORK UNIT NUMBER

7. PERFORMING ORGANIZATION NAME(S) AND ADDRESS(ES)

Trustees of Boston College
Boston College
140 Commonwealth Ave.
Chestnut Hill, MA 02467

8. PERFORMING ORGANIZATION REPORT NUMBER

9. SPONSORING / MONITORING AGENCY NAME(S) AND ADDRESS(ES)

U.S. Army Medical Research and Development Command
Fort Detrick, Maryland 21702-5012

10. SPONSOR/MONITOR'S ACRONYM(S)

11. SPONSOR/MONITOR'S REPORT NUMBER(S)

12. DISTRIBUTION / AVAILABILITY STATEMENT

Approved for Public Release; Distribution Unlimited

13. SUPPLEMENTARY NOTES

14. ABSTRACT

Forward deployed military units have a critical need for a robust, low cost, easy to use diagnostic system providing real-time, quantitative, and multiplex capability of identifying biomarkers for infectious disease, including tuberculosis. This is a project to develop a new diagnostic device for detection of a tuberculosis biomarker based on a novel "plasmonic halo" effect. Various halo nanodevices using a set of chosen metals and dielectrics were simulated and fabricated, and their plasmonic-optical response / sensitivity characterized. A major finding is that a modified structure showed promise for response in the near infrared, and the architecture may be amenable to rapid detection of viruses.

15. SUBJECT TERMS
Plasmonics, Biomarker, Quantum Dot, Biosensor, Finite Element Modeling, Bioassay, Index of Refraction

16. SECURITY CLASSIFICATION OF:			**17. LIMITATION OF ABSTRACT**	**18. NUMBER OF PAGES**	**19a. NAME OF RESPONSIBLE PERSON**
a. REPORT	**b. ABSTRACT**	**c. THIS PAGE**			USAMRDC
U	U	U	Unclassified	16	**19b. TELEPHONE NUMBER** *(include area code)*

TABLE OF CONTENTS

1. INTRODUCTION

There is an acute, unmet need for low cost, rapid detection of tuberculosis, as well as biomarkers of other diseases and pathogens, in a broad range of health care applications, including routine point of care (PoC) clinical evaluation, real time diagnosis and detection of infectious disease in military personnel. A critical aspect of recognizing and controlling tuberculosis in military personnel, and in future epidemics, relies on the development of such diagnostics that can be quickly deployed at multiple sites. The current project aimed to develop a diagnostic device for active tuberculosis via detection of TB-specific biomarkers. In the short term, the technology aimed to provide a rapid assay for PoC detection of tuberculosis in urine, with future goals of detecting biomarkers in blood and breath. Fully developed, the assay could be applied to a range of infectious and noninfectious human diseases, potentially including cancer and infectious diseases.

2. KEYWORDS

Plasmonics; Biomarker; Biosensor; Sensitivity; Functionalize; Spectroscopy; Nanofabrication; Metal Nanoparticle; Plasmon-enhanced; Materials optimization; Photolithography; Electron microscopy; Finite Element Modeling; Bioassay; Index of Refraction

3. ACCOMPLISHMENTS

Major goals of the project:

The main goal of the project was to develop a device that can quantitatively and with high sensitivity detect the presence of TB-specific biomarkers in solution (*i.e.,* urine or blood) in a compact, plasmonic halo device. The specific concept is that the optical responses of these specific biomarkers will be characterized in advance, and then plasmonic halo drumhead devices will be custom-designed and fabricated based on those response characteristics. Upon narrow-band illumination at or near an absorption peak of the target molecule or tethered light absorber/emitter, with that molecule resident in the near electromagnetic field of the drumhead surface, a detectable change in the transmission intensity arises. This change, corresponding to the presence of the target biomarker, is detected via a change in photocurrent in a proximate photodiode. The general concept is that this scheme can be applied to a wide range of disease biomarkers, in addition to tuberculosis. High specificity for such a device is provided by matching the drumhead halo structure's resonant mode(s) with the target biomarker's absorption peak(s), while high sensitivity is aided by the extreme sensitivity of photodiode detectors. As individual drumhead devices are only a few micrometers in size, the scheme is readily amenable to multiplexing, such that combinatorial analysis (multiple absorption peaks toward fingerprinting an individual target simultaneous to multiple molecular targets) is straightforward.

Specific Aims:

Aim 1: Select molecular targets
– Milestone 1a: Identify candidate biomarkers from a pool of emerging TB antigens, including LAM, ESAT6 and CFP10. LAM antigen has been chosen. (100% complete)
– Milestone 1b: Identify at least two anti-LAM antibodies from a pool of commercially-available monoclonal- and polyclonal- specific LAM antibodies. We have identified NR-13811 and NR-13812 monoclonal anti-mycobacterium tuberculosis LAM, Clone CS-35 (produced *in vitro*). (100% complete)
– Milestone 1c. Confirm sensitivity and specificity of anti-LAM antibodies on metal-attached surfaces via conventional SPR. (75% complete)
Aim 2: Simulate/model response of plasmonic halos
– Milestone 2a. Complete 2nd generation halo computer models. (100% complete)
– Milestone 2b. Complete prototype portable light source & light detector that could be used for halo measurements. (100% complete)
Aim 3: Fabricate plasmonic halo structures
– Milestone 3. Demonstrate proof-of-concept of halo-based detection of TB antigen above antigen-free control sufficient to warrant further development. (80% complete)

Major Activities and Significant Results

In this project, the project team modeled, made and measured plasmonic halo devices in terms of their optical response in the presence of proxy biological targets. Halo structures were optimized by characterizing their performance when biofunctionalized with known analytes and antigens, with the anticipation of transferring to a molecular target once the detection scheme has been finalized.

Finite Element Methods COMSOL and CST were used to model and simulate the response of halo structures to incident light without and with a biological target immobilized on the surface of the halo structure metal. To this end, the 'standard' drumhead halo, a modified drumhead, and a 'bulls-eye' structure were modeled. Simulations were extended to the near and mid infrared regimes, with the intention of identifying structure-material-based resonant peaks that may coincide with absorption resonances intrinsic to target macromolecules.

The bulls-eye plasmonic halo structure is shown in Figure 1, in four different views: an electron microscope image (SEM), a COMSOL simulation of the electric field due to plasmonic interactions along with metal surfaces, and atomic force microscope (AFM) image of the structure, and an optical microscopic image.

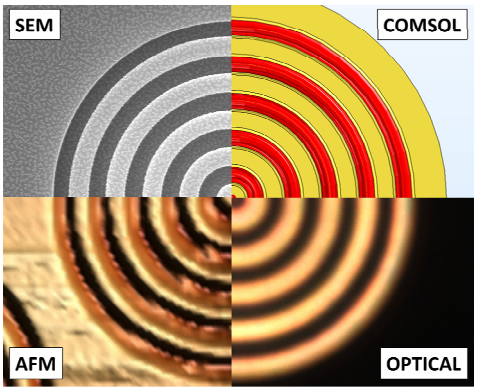

Figure 1. 'Bulls-eye' plasmonic halo structure displayed four ways. The overall diameter is approximately 10 μm.

Using modeling to predict and optimize the halo device structure and performance, devices were fabricated and tested under dry and biologically-relevant conditions. Figure 2 reproduces data for a series of devices, where the bulls-eye gap size was systematically varied, and the resulting optical transmittance recorded. The purpose of this study was to identify the dominant/characteristic absorbance and transmittance features resulting from plasmonic interactions, toward identification of size structures that optimize sensitivity.

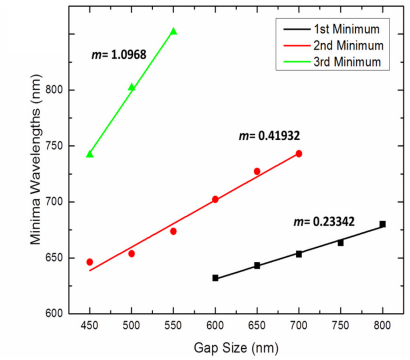

Figure 2. Varying feature size of bulls-eye plasmonic halo structure, showing wavelengths of sequential minima in transmittances showing systematic characteristics. Index *m* refers to nominal mode number.

For further characterization of sensitivity with respect to changes in index of refraction of the medium along the plasmonically-active surfaces (i.e. the base and side-walls as shown in several figures above), a particular transmittance feature (a local maximum) was monitored as the liquid medium was systematically varied. This variation led to a systematic variation of the refraction index. As such, a sensitivity in units of peak wavelength change per refractive index unit (RIU) could be calculated. Figure 3 below shows representative data.

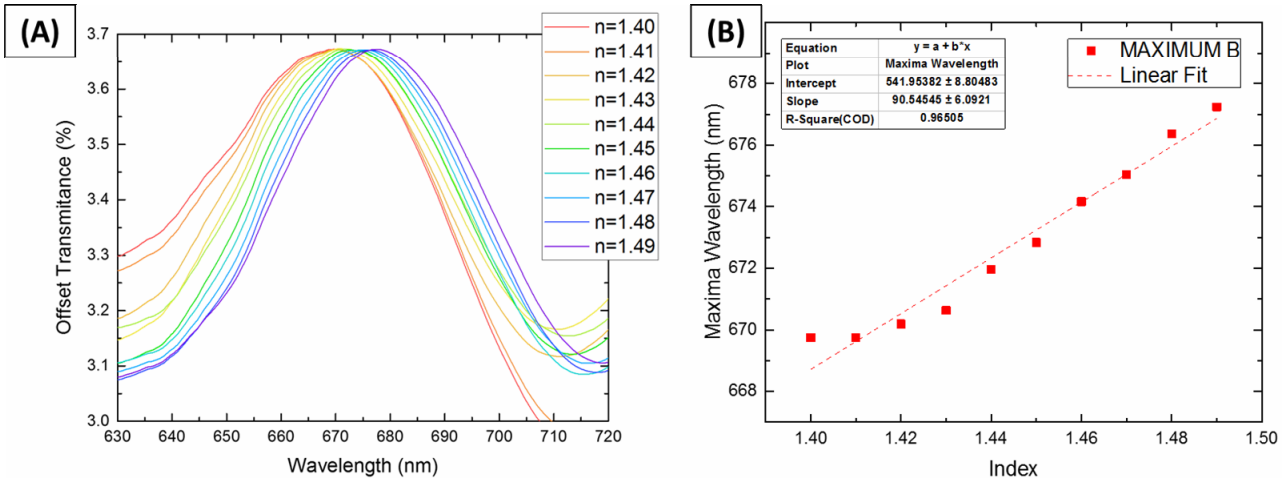

Figure 3. Transmittance maxima of 650 nm gap bulls-eye sample for different refractive index immersions. (B) Plot of maximum wavelength vs. RIU. The slope is a common value of sensitivity used in literature, here ~100 nm/RIU.

Confirming that there is a shift in transmittance with a change of refractive index of the medium in the vicinity of the halo, a biofunctionalization scheme was implemented to test this as a sensor. A schematic of the functionalization scheme is shown below. In step (a), the sample is immersed in a physiological solution of similar composition to the solution used in subsequent steps, e.g. PBS. In step (b), thiol-conjugated streptavidin (SA-thiol) is added to the sample. The thiol conjugate forms a strong bond to the Au surface and while the binding mechanism remains fully agreed upon, the binding strength has been quantified. In step (c), biotin-conjugated immunoglobin G (biotin-IgG) is added to the sample, facilitating the immobilization of IgG antibodies through the streptavidin-biotin binding. The biotin is conjugated to the Fc region of IgG thereby facilitating the steric availability of the fabrication region, which is specific to the targeted antigen. In step (d), the targeted antigen is added and is captured by the IgG. In step (e), the final configuration is measured for both wet and dry cases.

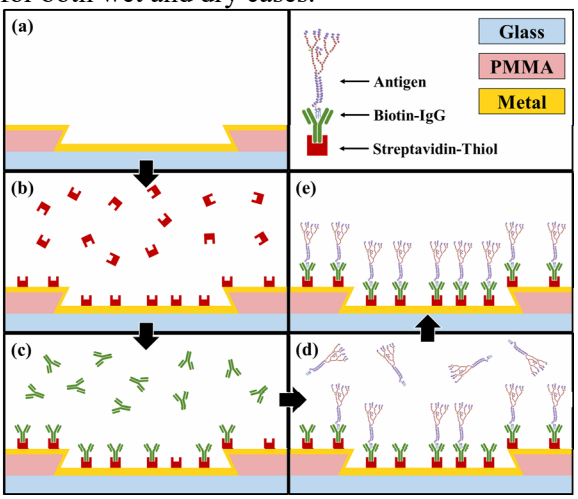

Figure 4. Antigen capture schematic. (a) baseline structure with physiological liquid, (b) + SA-thiol, (c) + biotinylated-IgG specific to targeted antigen, (d) + antigen, and (e) record final configuration.

Experiments were conducted to show the immobilization of biotinylated-IgG for a sample with SA-thiol compared with a control sample with SA-thiol. Figure 5 shows transmittance spectra for incident white light through arrays of a bullseye with corresponding gap size 400 nm, 500 nm, 600 nm, and 700 nm. These samples have Au metallic layers and were measured with an Ocean Optics USB2000 spectrometer.

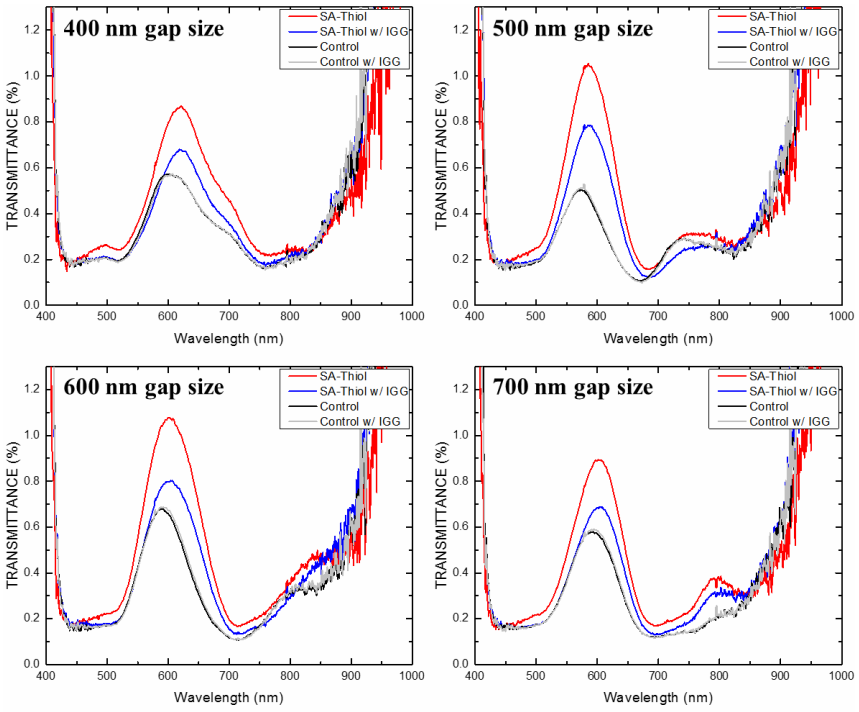

Figure 5. Transmittance before and after IgG. Bullseye arrays of different gap sizes for 2 separate chips (8 regions in total). For each sizing, spectra were measured before and after the addition of biotin-IgG to a sample with previously added SA-thiol and a control sample without previously added SA-thiol.

There were observable differences in the transmittance for the sample with SA-thiol versus relatively no change for the control sample. The change in the SA-thiol-laden sample predominately preserved the wavelengths of the spectral features and therefore is not consistent with the redshift anticipated for a surface plasmon mediated changed. Additionally, since the samples were made with Au, there is a falsely inflated peak in transmittance between 500 nm and 700 nm, indicating a possible source of surface plasmon dissipation. There is a consistent observable difference in the samples with and without SA-thiol before the addition of IgG, as is expected due to the immobilization of the SA-thiol.

Similar tests were performed for different samples and equipment, primarily to investigate the potential impact of a more sensitive spectrometer. An experiment was run adding PBS to a sample, then adding SA-thiol, and finally adding biotin-IgG. While there is a discernable shift from the binding of SA-thiol, the shift from the IgG was in the opposite direction than SPR interaction would indicate, likely due to the dissociation of unbound SA-thiol on the sample surface.

Detection of a fluorescent protein perCP (peridinin-chlorophyll-protein, a 35.5 kDa fluoresc-ent complex was also attempted. There was, unfortunately, insufficient difference between SA-thiolated halos and SA-thiol+perCP halos.

Since facile detection of biotin-IgG binding was not evident, it was concluded that this combination of structure, biological assay and detection method was not capable of sufficiently sensitive biofunctionalized biosensing. As such, efforts were shifted to signal enhancement schemes away from the visible and into the infrared regime.

Near-infrared results

Simulations of plasmonic halos in the near IR range of frequencies were performed. Figure 6 shows changes in transmittance of a halo when a simulated monolayer of viruses is immobilized on the active halo surface (green), versus no virus inclusion (red). As can be seen, the transmittance near 2350 nm wavelength increases by about 400% with target inclusion. Moreover, there are potentially even larger changes near 1600 nm and 1800 nm wavelengths, where the transmittances change from nearly undetectable to readily detectable levels. Similar changes are observed in the reflectance simulation, Figure 7: a nominal 300% relative increase at 1820 nm, and a 70% absolute decrease near 2350 nm.

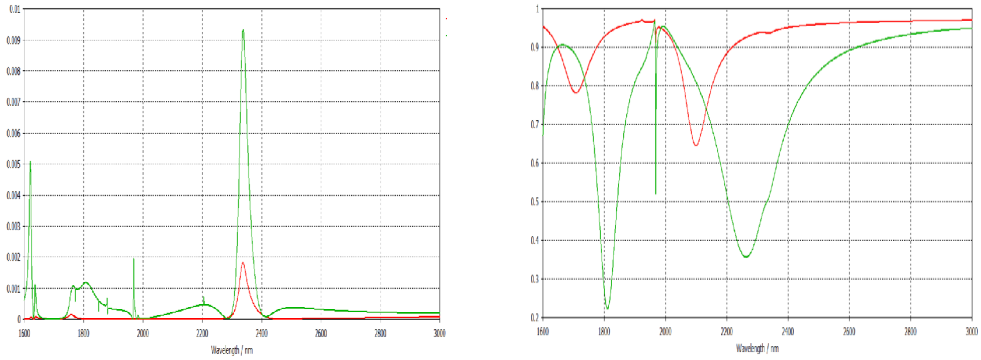

Figure 6. (**left**) Transmittance simulation in a plasmonic halo microstructure in the near IR, with (green) and without (red) monolayer coverage of a virus. **(right)** Reflectance simulation in a plasmonic halo microstructure in the near IR, with (green) and without (red) monolayer coverage of a virus.

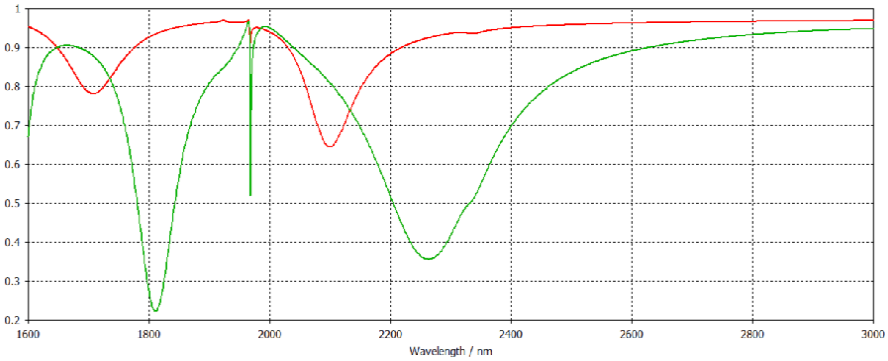

Figure 7. Reflectance simulation in a plasmonic halo microstructure in the near IR, with (green) and without (red) monolayer coverage of a virus.

Figure 8 below shows the parameters of the halo structure for the IR domain.

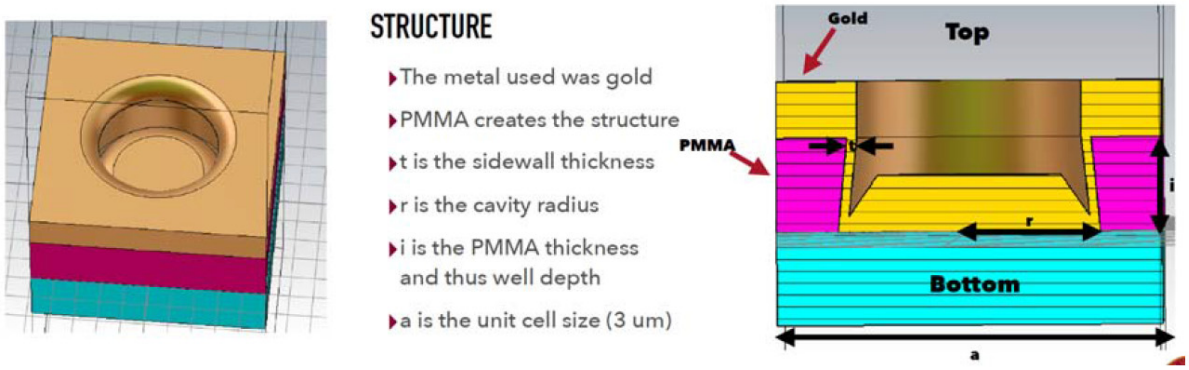

Figure 8. Structural parameters of plasmonic halo dimensioned for IR response.

In the simulations, we first modeled the sensitivity of the IR response on the halo radius (**r** in the figure above). As anticipated, there was only small dependence on **r**, within the range tested, as shown below in Figure 9.

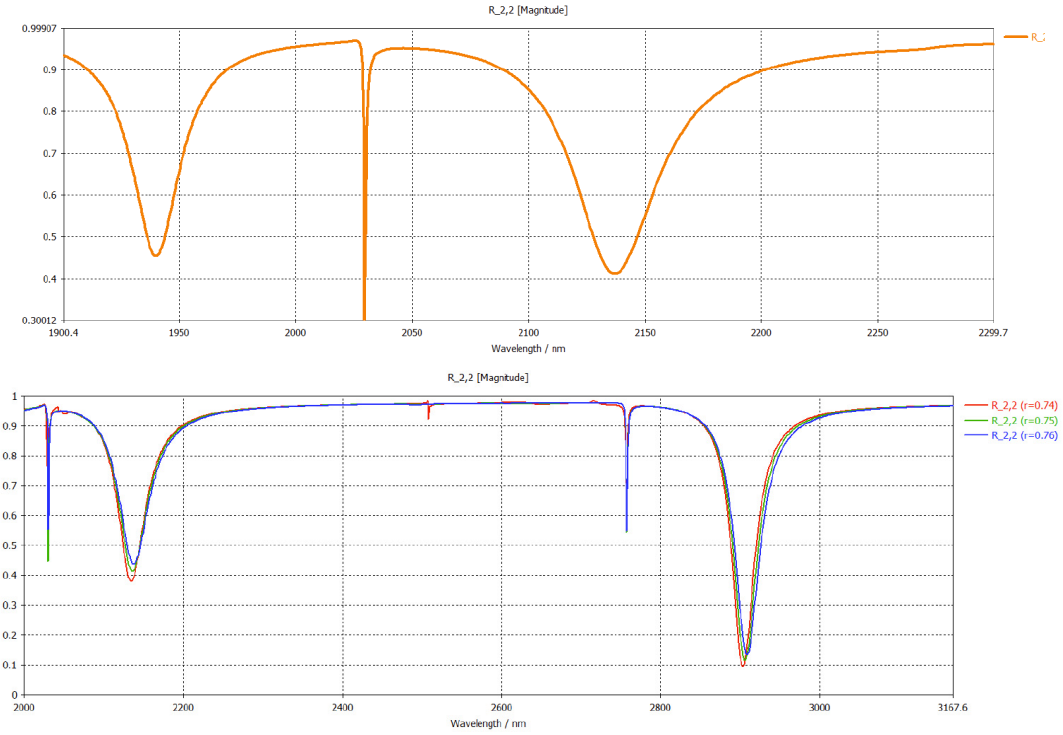

Figure 9. Infrared response of plasmonic halos with varied halo base radius.

We then concentrated on the 1,940 and 2,040 nm absorption peaks (reflectance minima) and tested via simulation the dependence on analyte thickness, a proxy for target quantity or volume. These results, in Figure 10, indicate a strong sensitivity, suggesting this a plasmonic halo of these dimensions operating in this range of IR frequencies could yield a functioning device.

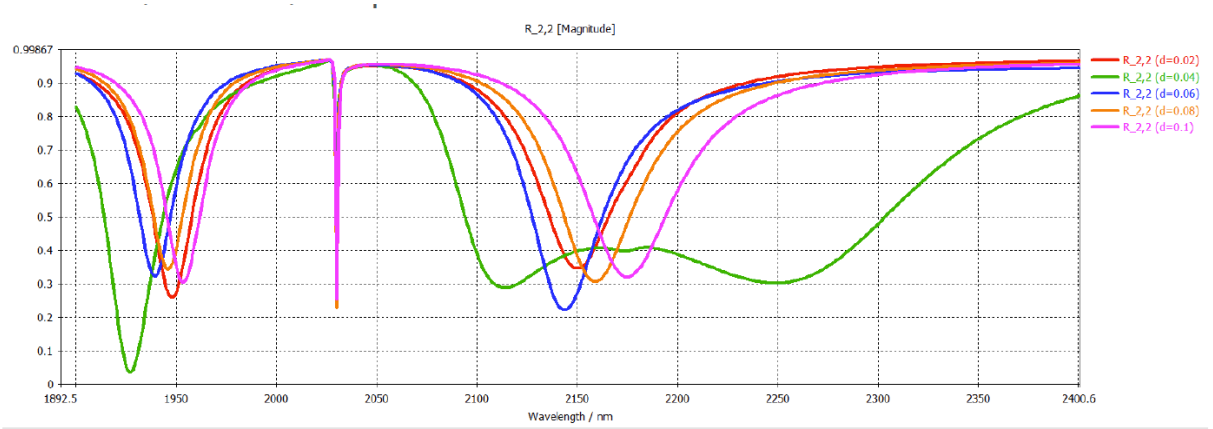

Figure 10. Infrared response of plasmonic halos with varied thickness dielectric filling, a proxy for quantity of molecular target quantity. The thickess was varied from 20 nm to 100 nm, as indicated in legend (in microns).

We then tested fabrication of IR-scale halo devices via e-beam nanolithography. SEM images of an EBL dose test are shown below.

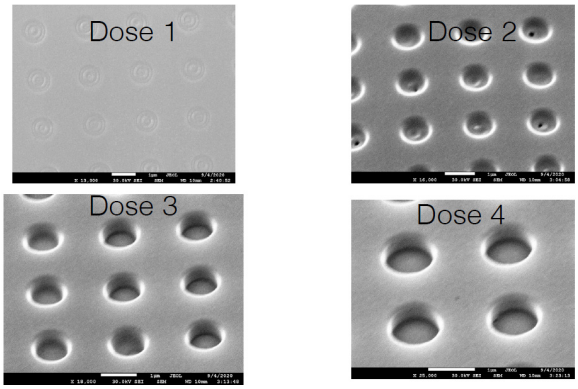

Figure 11. SEM images of electron beam lithography dose test for fabrication of IR-scale plasmonic halo devices.

Representative IR response data for the dose 3 & 4 halo structures are shown in Figure 12. As expected, a resonant absorption peak, represented here as a reflectance minimum centered near $\lambda = 1.5$ μm, was observed. Unlike the simulations, however, a 2nd peak, corresponding to a higher resonant mode, was not detected.

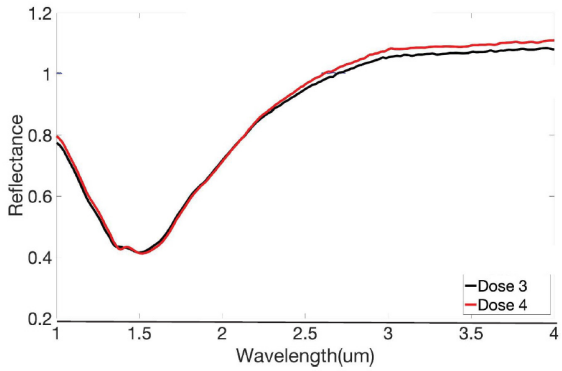

Figure 12. Infrared reflectance of IR-scale plasmonic halo devices, showing anticipated absorption peak near 1.5 μm wavelength.

Conclusions

While protocols for modeling, device fabrication, conjugation chemistry, and measurement capabilities of this project have been established, the performance of the plasmonic halo devices has ultimately proven underwhelming. To remind, the core idea is that resonant standing plasmon waves are wavelength-shifted when target molecules are captured onto the halo structure surface in such a way as to be resident in the significantly enhanced magnitude near electric field provided by the localized plasmon. Thus, even though the dielectric constant of the captured entity may differ only slightly from its ambient medium, the difference is amplified. This indeed occurs, and is measurable using devices appropriate for optical wavelengths, we anticipated better performance than the results obtained. This led us to investigate the near infrared, as reported herein. As in the case of the optical range, simulations in the IR showed promise, with substantial resonance changes predicted for small capture analyte volume. However, utilization of fabricated devices that are appropriate for near infrared wavelengths again showed negligible differences upon target analyte inclusion compared to control devices.

Opportunities for training and professional development the project has provided

Four undergraduate students were involved with this project, and thus had the opportunity for training on scientific equipment, conducting experiments, preparing and presenting experimental results, and studying related materials in both physics and biology. The training and professional development for two graduate students involved was also extensive. These opportunities included the advising of undergraduate research activities, advancing software skills in data analysis and computer modeling, proposing and presenting design of experiments, directing and executing of experiments, designing and producing samples using an array of state-of-art cleanroom technologies, disseminating research at national scientific conferences, and preparing results to publish to the broader scientific community. One graduate student incorporated this work into a Ph.D. thesis.

How results were disseminated to communities of interest

–No conferences attended due to covid.

Plans during the next reporting period to accomplish project goals

4. IMPACT

Impact on the development of the principal discipline(s) of the project

The diagnostic nanodevice developed, which relies on detection of specific human disease biomarkers, was meant to address an unmet need for low cost, rapid detection of active tuberculosis. The technology aimed to provide a rapid assay for PoC detection of disease markers in blood and urine; however the technology may potentially be scaled to detect biomarkers in breath. In the long term, the developed assay can be applied to a wider range of infectious and noninfectious human diseases. Fully developed, the research can become a foundation for future effort aimed at emerging infectious diseases to protect our military, with eventual benefit to those in low-resource areas where access to clinical infrastructure and technology is limited, such that accurate, PoC detection is highly desired.

Impact on other disciplines

Integrating the nanofabrication techniques and materials with the biological schemes and assays necessary to achieve our targeted novel detection mechanisms and sensitivities would have a significant impact on the interdisciplinary fields of global public health, biomedicine and nanotechnology. Our research solutions to the problems of developing an impactful biosensing device can be an important to others in this growing field of interdisciplinary science.

Impact on technology transfer

N/A

Impact on society beyond science and technology

Fully developed, the research could become a foundation for future effort aimed at emerging infectious diseases to protect not only US military personnel and those in low-resource areas where access to major infrastructure and technology is limited, but to conventional clinical settings in hospitals and doctors' offices, thus providing large public health benefit.

5. CHANGES/PROBLEMS

Changes in approach and reasons for change

Computer simulations led us to investigate, in addition to the bulls-eye structures, modified halo structures that show resonance features in the near infrared. These features suggested that these structures can be more sensitive as plasmonic biosensors than the original design,

Actual or anticipated problems or delays and actions or plans to resolve them

Covid-19 had the largest impact with respect to delays.

Changes that had a significant impact on expenditures

A 2nd graduate student, Mark Schiller, began work on the project in 2020. Via modeling and simulation, he discovered and pursued the near-IR detection scheme discussed above.

Significant changes in use or care of human subjects

Nothing to Report

Significant changes in use or care of vertebrate animals

Nothing to Report

Significant changes in use of biohazards and/or select agents

Nothing to Report

6. PRODUCTS

- **Publications, conference papers, and presentations**

– Contributed talk by Boston College graduate student Luke D'Imperio at the APS (American Physical Society) March meeting in Boston, March 5, 2019 "Plasmonic Halos Towards Molecular Sensing of Disease Biomarkers" in *Session H23: Physics in Medicine: Imaging, Therapy, and Disruptions on the Horizon*, coauthors Juan M. Merlo, Chaobin Yang, Yitzi M. Calm, Megi Maci, Michael J. Burns, Timothy Connolly, Thomas C. Chiles, Michael J. Naughton. *https://meetings.aps.org/Meeting/MAR19/Session/H23.5*

- **Other publications, conference papers and presentations**

Nothing to Report

- **Website(s) or other Internet site(s)**

Nothing to Report

- **Technologies or techniques**

Nothing to Report

- **Inventions, patent applications, and/or licenses**

Nothing to Report

- **Other Products**

Nothing to Report

7. PARTICIPANTS & OTHER COLLABORATING ORGANIZATIONS

Name:	**Michael J. Naughton, Ph.D.**
Project Role:	PI
ORCID ID:	0000-0002-6733-2398
Nearest person month worked:	1
Contribution to Project:	Prof. Naughton has supervised all aspects of the work.
Funding Support:	This award
Name:	**Thomas C. Chiles, Ph.D.**
Project Role:	Co-PI
Nearest person month worked:	1
Contribution to Project:	Prof. Chiles has co-supervised the biological aspects of the work.
Funding Support:	This award
Name:	**Timothy Connolly, Ph.D.**
Project Role:	Co-PI
Nearest person month worked:	1
Contribution to Project:	Dr. Connolly has contributed to the SPR experiments, bioassay development and co-supervised the bio/chemical aspects of the work.
Funding Support:	N/A
Name:	**Luke D'Imperio**
Project Role:	Graduate Student
ORCID ID:	N/A
Nearest person month worked:	28
Contribution to Project:	Dr. D'Imperio wass a physics graduate student that worked on the project, including modeling and simulation, fabrication and testing.
Funding Support:	This award
Name:	**Mark Schiller**
Project Role:	Graduate Student
ORCID ID:	N/A
Nearest person month worked:	11
Contribution to Project:	Mr. Schiller is a physics graduate student that has worked on the project, primarily on modeling and simulation
Funding Support:	This award
Name:	**Victoria Gabrielle**
Project Role:	Graduate Student
Nearest person month worked:	1
Contribution to Project:	Ms. Gabrielle is a physics graduate student involved with the project. She has been involved with device microfabrication, and biochemical aspects of the work.
Funding Support:	This award

Change(s) in the active other support of the PD/PI(s) or senior/key personnel since the last reporting period

Nothing to Report.

Other organizations were involved as partners

Nothing to Report.

8. SPECIAL REPORTING REQUIREMENTS

COLLABORATIVE AWARDS: *N/A*

QUAD CHART: *attached*

9. APPENDICES:

Curriculum vitae of M. J. Naughton